Journal of Materials Science: Materials in Electronics (2018) 29:8380–8389
https://doi.org/10.1007/s10854-018-8849-y

Assembly of carboxylated zinc phthalocyanine with gold nanoparticle for colorimetric detection of calcium ion

Xuefei Zhou[1] · Kun Jia[1] · Xiaohong He[1] · Shiliang Wei[1] · Pan Wang[1] · Xiaobo Liu[1]

Received: 31 December 2017 / Accepted: 1 March 2018 / Published online: 5 March 2018

Abstract
A series of water-soluble carboxylated zinc phthalocyanine (ZnPc-COOH) were obtained from a facile hydrolyzation of terminating nitriles groups of zinc phthalocyanine synthesized via bisphthalonitrile based precursor. After the gold nanoparticles (Au NPs) with positively charged surfactant CTAB was added to as-prepared ZnPc-COOH solution, the electronic interaction between them would contribute to the tunable conjugate of Au NPs/ZnPc-COOH and lead to a red-shifted absorption peak in UV–Vis spectrum. Specially, both of the amount of phthalocyanine rings and concentrations of ZnPc-COOH would make a big difference in the interaction with Au NPs. In the presence of different metal ions, the ZnPc-COOH/Au NPs aqueous solution revealed selective response to Ca^{2+}, leading to an increased aggregation extent and the naked eye visualized color change. The further experiment revealed that the red-shift was accessible in a wide concentration range of Ca^{2+}, and the red-shift degree was proportional to the concentration of Ca^{2+} in the range of 2–8 μM with a limit of detection defined as 1 μM. Combing the photosensitivity of ZnPc-COOH and localized surface resonance plasmon of Au NPs, this label-free probe would provide a potential application in colorimetric detection and photosensitization under physiological environment.

1 Introduction

Phthalocyanine (Pc) and related derivatives containing the delocalized 18π-electron aromatic skeleton exhibited high structure stability [1], broad absorption band in the visible region and high excitations quantum yield [2], which lay the foundation for different applications in chemical sensors [3], photodynamic therapy (PDT) [4], non-linear optical devices [5], photochemical catalysts [6, 7], etc. Particularly, the inherent π–π stacking tendency of phthalocyanine (Pc) usually induces different aggregation states along with distinctive optical properties. Previously, we have systematically investigated the photophysical properties and intermolecular charge transfer of ZnPc in different structures and aggregation states, which revealed that both of the fluorescence emission intensity and wavelength of specific ZnPc could be modulated by changing the aggregation states based on ACQ and AIE-dominated framework [8, 9]. Nevertheless, their rigid and planer structure of phthalocyanine (Pc) would inevitably give rise to the low solubility in organic solvents and aqueous solution [10], while most biological and environment processes were proceed in aqueous medium and the low solubility of phthalocyanine would largely restricted their application [11, 12]. To relieve the inherent intermolecular aggregation property of Pc, the two strategies derived from tailorable structure of phthalocyanine inspired were employed to improve their solubility [13], namely the modification of substituent group into peripheral or axial position of the macrocycle and choosing proper coordinating metal ion to the central cavity [14, 15]. Generally, introducing hydrophilic substituents to the periphery of phthalocyanines would lead to a series of water-soluble phthalocyanine, including anionic (sulfonated or carboxylated), cationic (quaternized), non-ionic (polyethylene glycol substituted, carbohydrate substituted) and even zwitterionic phthalocyanine [16, 17]. Accordingly, the bisphthalonitrile was considered as a suitable precursor for synthesizing soluble phthalocyanine, due to the fact that cyano group in the

Electronic supplementary material The online version of this article (https://doi.org/10.1007/s10854-018-8849-y) contains supplementary material, which is available to authorized users.

✉ Kun Jia
jiakun@uestc.edu.cn

✉ Xiaobo Liu
liuxb@uestc.edu.cn

[1] Research Branch of Advanced Functional Materials, School of Materials and Energy, University of Electronic Science and Technology of China, Chengdu 611731, People's Republic of China

periphery of phthalocyanine (Pc-CN) could be hydrolyzed into phthalic acid based compounds in strong basic solution leading to a carboxylated phthalocyanine (Pc-COOH) [18, 19]. Furthermore, the soluble Pc-COOH with peripheral carboxylate would be potential in combining more functional materials, such as metal ions and functional groups, for further application [20, 21].

As a remarkable member of the nano-materials family, gold nanoparticles (Au NPs) possessed intriguing optical and electronic properties and have been widely used as sensor [22, 23], catalysis [24, 25], drug delivery agent [26], etc. Due to the nanoscale confinement of electrons on the surface, Au NPs exhibited extremely high extinction coefficient (10^8–10^{10} M^{-1} cm^{-1}) and obvious localized surface plasmon resonance (LSPR) band, which was dependent on the size of particles and dielectric constant of surrounding environment, and allowed selective detection to even small amount of analyte [27, 28]. In addition, the advantages of Au NPs, such as the large surface to volume ratio, facile synthesis and functionalization method also promoted the practicability of Au NPs-based sensors [29]. Especially, the well dispersed Au NPs in aqueous solution was red and the conventional SPR peak located at visible region around 530 nm, whereas the aggregated Au NPs solution would appear purple or blue with a red-shifted LSPR peak, and the visible color change made the Au NPs competent to act as colorimetric sensor [30]. Metal ions chemosensors has attracted enormous attention due to the crucial role in various biological and environmental processes, like that Ca^{2+}, Zn^{2+}, Mg^{2+} would help to prevent cytotoxicity while the accumulation of Pb^{2+}, Cd^{2+}, Hg^{2+}, As^{2+} and Al^{3+} can lead to serious disorder [31]. For instance, Li and co-workers utilized Au NPs as a probe for colorimetric detection of cysteine with the help of Cu^{2+} acting as cross-linking agent for cysteine-coated Au NPs [32]. Zhang and his co-worker used the conjugated mercaptosuccinic (MSA) and Au NPs to interact with Ca^{2+} via the carboxylic group of MSA, which resulted in color change and red shift of SPR peak [33]. Kim et al. functionalized Au NPs with a calcium-binding protein calsequestrin (CSQ), and was capable to work as colorimetric calcium sensor based on aggregation by interacting with Ca^{2+} [34].Obviously, the Au NPs was quite sensitive to metal ions and capable to function as a colorimetric sensor.

In our previous work, a water soluble carboxylated zinc phthalocyanine (ZnPc-COOH) based on zinc phthalocyanine containing cyano groups (ZnPc-CN) was firstly synthesized, which was then assembled with the nanoscale template gold nanorods (Au NRs) to obtain water-soluble ZnPc-COOH/Au NR nanoconjugates with a recovered NIR fluorescence as well as improved singlet oxygen quantum yield [18]. Based on these work, we further explored the interaction between water-soluble zinc phthalocyanine and gold nanoparticles, and evaluated the optical response of Au NPs/ZnPc-COOH to different metal ions in this work. Firstly, three zinc phthalocyanine (ZnPc-CN) with different ring contents have been synthesized by adjusting annulation reaction time interval of 6, 10, 20 h, respectively. By hydrolyzing the peripheric nitrile group into carboxyl, the hydrophobic ZnPc-CN successfully transformed into water-soluble zinc phthalocyanine (ZnPc-COOH). Moreover, the CTAB-stabilized Au NPs was assembled with ZnPc-COOH to obtain the ZnPc-COOH/Au NPs conjugate showing specific optical response to Ca^{2+}.

2 Experimental

2.1 Materials

4,4′-Bis(3,4-dicyanophenoxy)phenolphthalein was synthesized according to our previous work [18], zinc chloride ($ZnCl_2$), ammonium molybdate, methanol, *N,N*-dimethylformamide (DMF), tetrahydrofuran (THF), petroleum ether (C60–C90), silica gel, sodium hydroxide ($NaBH_4$), ascorbic acid (AA), chloroauric acid ($HAuCl_4$), calcium chloride ($CaCl_2$), aluminum chloride ($AlCl_3$), ,silver nitrate ($AgNO_3$), ferric chloride ($FeCl_3$), ferric chloride ($FeCl_2$), mercury chloride ($HgCl_2$), potassium chloride (KCl) ,sodium chloride (NaCl), copper chloride ($CuCl_2$),lead nitrate ($PbNO_3$), magnesium chloride ($MgCl_2$) and nickel chloride (LiCl) were received from Sinopharm chemical reagent. Cetyltrimethylammonium bromide (CTAB) was received from Shanghai Aladdin biological technology Co. Ltd. Deionized water was used in the experiment. All the compounds were used as received without further purification.

2.2 Synthesis of ZnPc-CN and ZnPc-COOH

The zinc phthalocyanine (ZnPc-CN) was synthesized according to our previous work [20], which was obtained after a reflux of 4,4′-bis(3,4- dicyanophenoxy)phenolphthalein (2.28 g, 4 mmol), zinc chloride (0.136 g, 1 mmol) and ammonium molybdate (10 mg) in 10 mL *N,N*-dimethylformamide (DMF) under vigorous stirring for specific time. After a precipitation in ddH_2O and purification in boiling methanol, the raw product went through further purification using a mixture of tetrahydrofuran and petroleum ether (volume ratio of 3:1) as an eluent. Finally, the purified green powder was obtained via rotary evaporating and vacuum drying. Herein, three ZnPc-CN samples distinguished each other by different annulation reaction time of 6, 10, 20 h and were denoted as ZnPc-CN-6, ZnPc-CN-10 and ZnPc-CN-20, respectively. The chemical structure of ZnPc-CN was characterized with ^{1}H NMR (DMSO-d6, 400 MHz): 8.11 (1 H, d, J 8.7), 8.02–7.84 (4 H, m), 7.72 (1 H, t, J 7.5), 7.45 (5 H, dd, J 13.0, 5.5), 7.24 (3 H, d, J 8.6), 3.34 (7 H, s), 2.50

(7 H, s). (see Fig. S1 in the Supplementary Materials). The water-soluble zinc phthalocyanine were obtained by the following procedure, 100 mg ZnPc-CN was refluxed in 30 mL NaOH (1 mol L^{-1}) aqueous solution at 100 °C with continuous stirring for 24 h. After the pH adjustment by HCl solution and precipitation using methanol, the ZnPc-COOH was incubated at room temperature for 12 h. The obtained ZnPc-COOH were denoted as ZnPc-COOH-6, ZnPc-COOH-10 and ZnPc-COOH-20, which were consistent with the former denotation. The chemical structure ZnPc-COOH was characterized with ^{1}H NMR (DMSO-d6, 400 MHz): 7.95 (1 H, t, J 13.3), 7.90–7.57 (2 H, m), 7.41 (2 H, d, J 8.6), 7.17 (4 H, t, J 13.0), 3.34 (4 H, s), 2.50 (3 H, s). (see Fig. S2 in Supplementary Materials). The thermal transition properties of ZnPc-CN and ZnPc-COOH were exhibited in Fig. S4, which certificated the microscopic H-type aggregates of ZnPc-COOH in aqueous solution.

2.3 Synthesis of gold nanoparticles

Gold nanoparticles (Au NP) were briefly prepared on the basis of seeding growth method which was developed by Nikoobakht and El-Sayed with a slightly modification [35]. The seed solution was achieved in a clean vial including the mixture of $HAuCl_4$ (2.5 mL, 1 mM), CTAB (5 mL, 0.2 M) and H_2O (2.5 mL), then, ice-cold $NaBH_4$ (0.6 mL, 10 mM) was injected to the mixture under magnetic stirring. The mixture turned to be brownish in 2–3 min and it would be stored at 25 °C for 2 h before use. Then, a dark yellow solution was prepared by mixing $HAuCl_4$ (1 mL, 10 mM) and CTAB (19 mL, 0.1 M), and it turned to be colorless after adding ascorbic acid (0.12 mL, 0.1 M), indicating the growth solution was achieved. Furthermore, the seed solution (320 µL) was added to the growth solution, the final solution was incubated at 28 °C for 12 h. Finally, the Au NPs solution was centrifuged at 14,000 rpm for 10 min and washed by deionized water once to remove unreacted reagent and some uneven particles.

2.4 Interaction between ZnPc-COOH and Au NPs

The synthesized Au NPs aqueous solution was diluted about 0.1 nM, then, 900 µL of the solution was added to a clean vial. Moreover, 100 µL ZnPc-COOH aqueous solution of definite concentration (0.0025, 0.005, 0.01, 0.02 mg mL^{-1}) were respectively incubated with the former Au NPs solution at room temperature to allow the interaction between positively charged Au NPs and negatively charged ZnPc-COOH. The interaction between ZnPc-COOH and Au NPs was monitored by UV–Vis spectrometer.

2.5 Procedure for colorimetric determination of cationic

According to the former experiment, the mixture containing ZnPc-COOH-10-2 (0.012 mg mL^{-1}) and Au NPs (0.1 nM) were chosen for further colorimetric analysis. A typical colorimetric analysis was realized by following steps. Firstly, 50 µL ZnPc-COOH and 900 µL Au NPs homogenized in a glass beaker. Then, 50 µL aliquots of aqueous Ca^{2+} ions with different concentration were mixed with 900 µL ZnPc-COOH/Au NPs solution in quartz cuvette. The final mixtures were stabilized for 5 min at room temperature before UV–Vis absorption measurements. The concentration of Ca^{2+} was quantified by the red-shift degree of the characteristic absorption peak of Au NPs in the ternary mixture. The selectivity of ZnPc-COOH/Au NPs towards Ca^{2+} were evaluated by testing the response of other metal ions, including Al^{3+}, Fe^{3+}, Cu^{2+}, Fe^{2+}, Mg^{2+}, Pb^{2+}, Ag^{+}, K^{+}, Na^{+}, Hg^{+}, Li^{+} at a concentration of 0.1 M.

2.6 Characterization

Fourier transform-infrared spectra were characterized with a Shimadzu 8400S FTIR spectrometer. The chemical structures were characterized with a Bruker AV II-400 spectrometer and the ^{1}H NMR (400 MHz) chemical shifts were measured relative to DMSO-d6 (H:d = 2.50 ppm) as the internal references. Thermal gravimetric analysis (TGA) was conducted with a TA Instruments TGA-Q50 under nitrogen atmosphere with a heating rate of 20 °C·min^{-1}.The thermal transition analysis were obtained on a differential scanning calorimetry Instrument (DSC, TA, Q100) under nitrogen atmosphere at a heating rate of 10 °C min^{-1}. The UV–Vis absorption spectra of synthesized Au NPs, ZnPc-COOH and ZnPc-COOH/Au NPs were characterized with a Persee TU 1901 UV–Vis spectrophotometer. The fluorescence spectra were recorded by using a conventional optical microscope (Motic, BA410E) coupled with a 405 nm laser, portable spectrophotometer. The morphology of synthesized Au NPs was characterized with transmission electron microscope (TEM, JEOL, JEM-2100F operating at 200.0 kV). The scanning electron microscope (SEM, JEOL, JSM-5900LV) was used to record the surface morphology of ZnPc-COOH and ZnPc-COOH/Au NPs. The photos of sample vial under visible and UV light were captured using a Nikon D7000 DSLR camera.

3 Results and discussion

To obtain the water-soluble zinc phthalocyanine, a bisphthalonitrile precursor was used to synthesize zinc phthalocyanine by a facile cycloaddition method [8]. As shown in

Scheme 1, three different cyano-terminated zinc phthalocyanines (ZnPc-CN) denoted as ZnPc-CN-6, ZnPc-CN-10 and ZnPc-CN-20 have been synthesized depending on the reaction time of bisphthalonitrile cycloaddition. After a one-step hydrolysis reaction, the peripheral nitrile groups on ZnPc-CN could turn to carboxyl realizing the water-soluble carboxylated zinc phthalocyanine (ZnPc-COOH), which was negatively charged and capable to detect or interact with positively charged materials, the corresponding ZnPc-COOH was obtained in the same method and denoted as ZnPc-COOH-6, ZnPc-COOH-10 and ZnPc-COOH-20, respectively. The ZnPc-CN in DMF solvent gave intense NIR fluorescence while the fluorescence of ZnPc-COOH disappeared in aqueous solution, as shown in Fig. S3.

The FTIR spectra corresponding to ZnPc-CN and ZnPc-COOH were displayed in Fig. 1a, b, the absorption band at 1779 cm^{-1} was corresponded to C=O stretching vibration of lactonic ring, and the characteristic absorption of the alternant C=N in the phthalocyanine ring was located at 1604 cm^{-1}. Besides, the bands at 1232–1390 cm^{-1} ascribed to skeletal vibrations while the absorption band at 2365 cm^{-1} belonged to –C≡N in the periphery of phthalocyanine ring, as shown in Fig. 1a. Specifically, more and more –C≡N has participated in zinc phthalocyanine ring as the cycloaddition time increased along with a decreased absorption band at 2365 cm^{-1} in the FTIR spectra. Moreover, the Fig. 1b indicated that the active –C≡N of ZnPc-CN got disappeared after the hydrolyzation in a strong base solution, which suggested that the peripheral cyano of ZnPc-CN has been completely hydrolysed to carboxyl. The TGA curves of all ZnPc-CN and ZnPc-COOH were collected under nitrogen atmosphere. As shown in Fig. 1c, the 5% weight loss

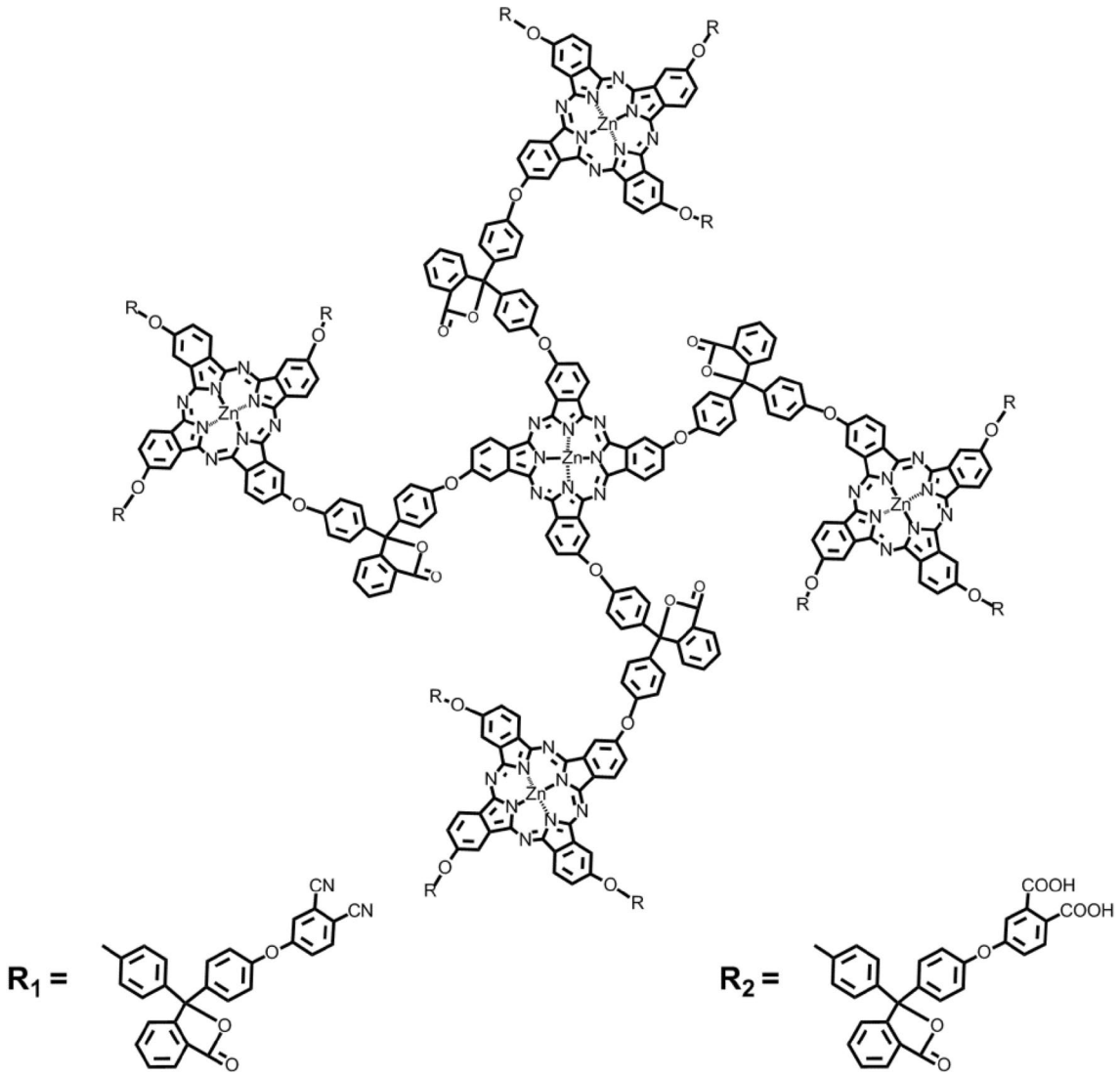

Scheme 1 The chemical structures of ZnPc-CN (R_1) and ZnPc-COOH (R_2)

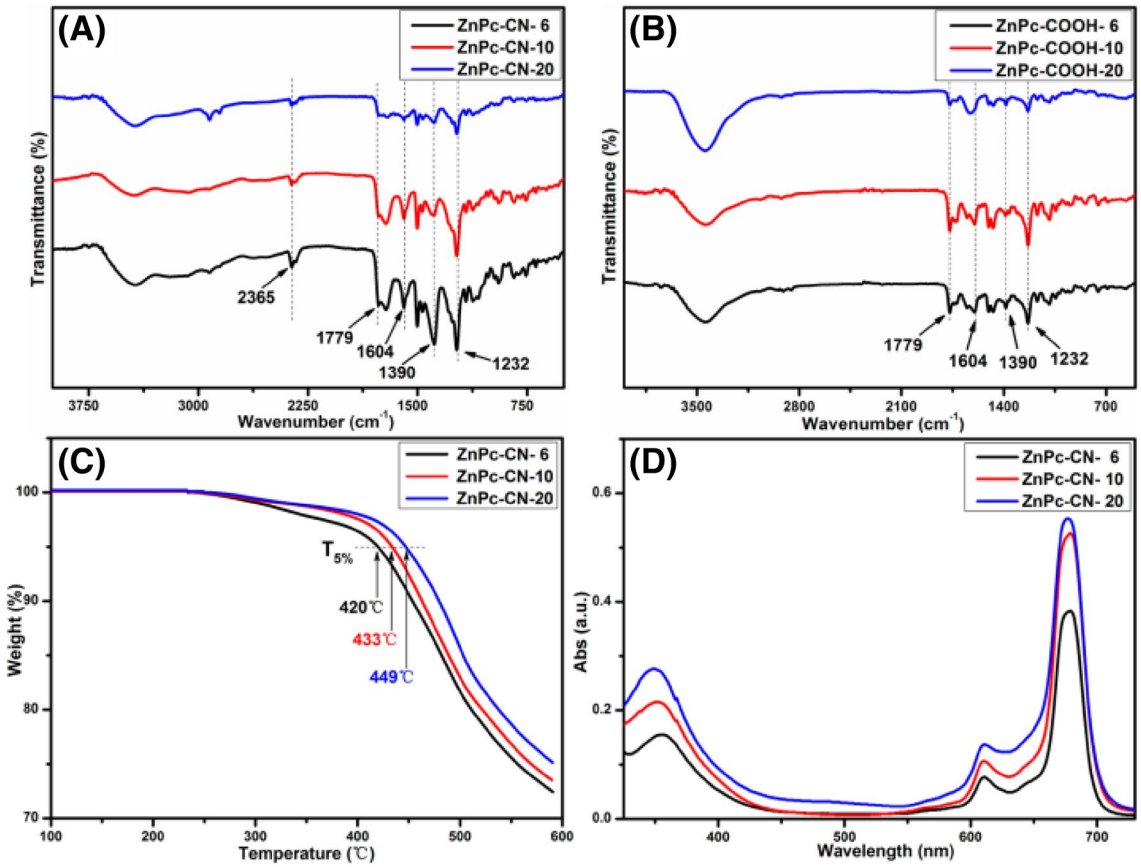

Fig. 1 FTIR (**a, b**), TGA (**c**) of ZnPc-CN and ZnPc-COOH, and UV–Vis spectra (**d**) of ZnPc-CN in DMF solvent

temperatures varied from 420 to 449 °C as the increase of cycloaddition time of ZnPc-CN, proving that the extended phthalocyanine structure exhibits better thermostability. It is well known that the two characteristic absorption bands of phthalocyanines are highly dependent on their molecular aggregation states. Given that phthalocyanine has characteristic conjugated π-electron aromatic structure, which would present an intense absorption band at near-infrared region, thus all of the three kinds of ZnPc-CN were dissolved at DMF solvent with the same concentration of 0.01 mg mL^{-1} for absorbance detection. As expected, the ZnPc-CN solution in DMF possessed good solubility and gave two typical absorption bands, namely the Soret band cantered at 355 nm and the main Q-band at 678 nm in combination with a weak vibronic shoulder at 610 nm, as shown in Fig. 1d. The linear relationship between concentration and absorbance in Fig. S5 indicated that the ZnPc-COOH in aqueous solution existed as H-type aggregates with high purity. On the basis of the absorption intensity at 678 nm, three ring contents of ZnPc in different cycloaddition times were calculated to be 36.61, 49.54 and 51.82% (see Supporting Information), respectively, and revealed that the ring contents gave an obvious increase with the cycloaddition times raise from 3 to 6 h, while a relatively slow increase was obtained with a prolonged cycloaddition time of 20 h. Furthermore, the increased absorption band at 678 nm in UV–Vis spectra was in accordance with the decreased absorption band at 2365 cm^{-1} in FT-IR spectra of Fig. 1a, both of which were due to the formation of extend phthalocyanine unit.

After a facile one-step hydrolysis of previously synthesized ZnPc-CN in NaOH solution, a new absorption spectra of ZnPc-COOH with a 14 nm blue-shifted and increased vibronic shoulder peak at 624 nm and obviously decreased Q band at 678 nm were detected, as shown in Fig. 2a. As mentioned previously, the absorption spectrum was closely related to molecular state, the alternation of absorption band should be attributed to the significant intermolecular interaction in the self-assembled nanostructure. On the other hand, the SEM image in Fig. 2b certificated that ZnPc-COOH exhibited the microscopic H-type aggregates in aqueous solution and the average diameter of the aggregates was detected around 250 nm, which lay a foundation for further sensing application in aqueous solution on the basis of specific morphology features. With this in mind, the gold nanoparticles (Au NPs) with CTAB as stabilizer were selected to modulate ZnPc-COOH for

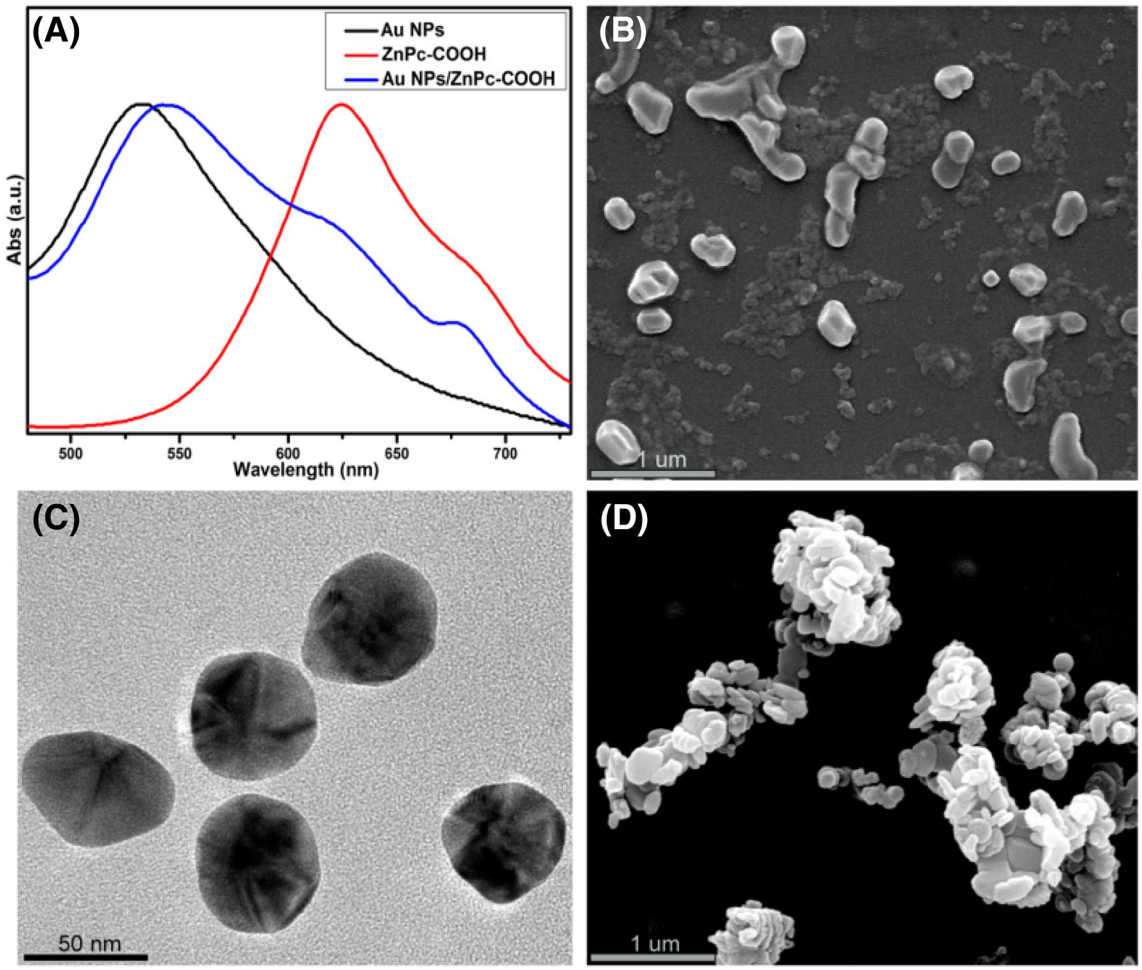

Fig. 2 The UV–Vis absorption spectra of synthesized Au NPs, ZnPc-COOH and ZnPc-COOH/Au NPs hybrid complex (**a**), and the SEM morphology of ZnPc-COOH (**b**), ZnPc-COOH/Au NPs (**d**) and TEM morphology of Au NPs (**c**), respectively

further application, for that the high sensitivity of Au NPs to microenvironment could be directly detected from UV–Vis spectra and the cationic surfactant CTAB would help Au NPs to assemble with ZnPc-COOH by electrostatic interaction. As displayed in Fig. 2a, the localized surface plasmon resonance (LSPR) wavelength of Au NPs was 534 nm, corresponding to the monodispersed and spherical Au NPs with a diameter of 50 ± 10 nm in size, as shown in Fig. 2c. Then, the monodispersed Au NPs was added to ZnPc-COOH aqueous solution under homogeneous mixing, resulting in prompt variation from microscopic morphology to detectable absorption spectra. The ZnPc-COOH/Au NR hybrid complex in Fig. 2d clearly exhibited the ZnPc-COOH H-type aggregates can be further assembled together via the electrostatic interaction with Au NPs. In addition, a red shift of the Au NPs absorption band from 534 to 553 nm also certificated the interaction between ZnPc-COOH and Au NPs, as the UV absorption spectra presented in Fig. 2a and it was believed that the high molar excitation coefficient of Au NPs has contributed to the detectable spectra variation.

To select appropriate Au NPs/ZnPc-COOH hybrid complex for further application, the ZnPc-COOH aqueous solution with different ring contents and concentrations were prepared and the interaction with Au NPs have been traced by UV–Vis spectrophotometer in detail, as shown in Fig. 3. On account of that the absorbance of phthalocyanine was in consistent with its ring content, herein ZnPc-COOH aqueous solution with different concentrations has been prepared on the basis of ring content. As shown in Fig. 3a, four groups of ZnPc-COOH-6 were denoted according to their increased concentration as ZnPc-COOH-6-1 (0.0045 mg mL^{-1}), ZnPc-COOH-6-2 (0.009 mg mL^{-1}), ZnPc-COOH-6-3 (0.018 mg mL^{-1}), ZnPc-COOH-6-4 (0.036 mg mL^{-1}), and different aggregation extent were contrasted after they were separately mixed with Au NPs (0.1 nM). The localized surface plasmon resonance (LSPR) peak of Au NPs was located at 534 nm, and a red shift to 541 nm was observed

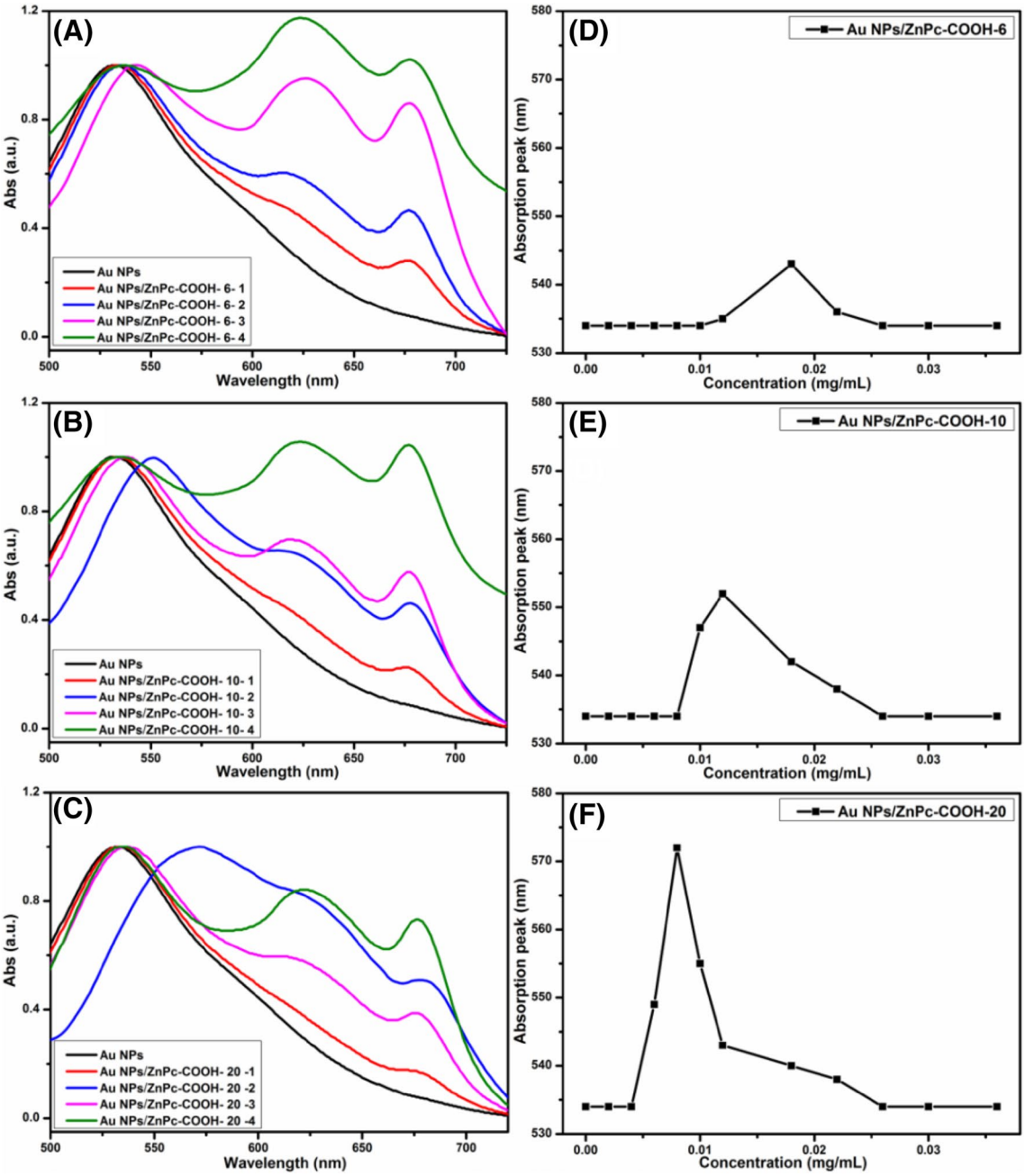

Fig. 3 The UV–Vis spectra (**a**–**c**) and absorption peak shift (**d**–**f**) of Au NPs interacted with ZnPc-COOH of different ring contents and concentrations

after adding the ZnPc-COOH aqueous solution in a concentration of 0.018 mg mL^{-1}. On the contrary, the electronic absorption spectra of Au NPs almost unchanged after mixing with ZnPc-COOH in other concentration. Therefore, it was believed that the positively charged Au NPs was capable to interact with negatively charged ZnPc-COOH under electrostatic interaction, but the ZnPc-COOH aggregate in low concentration would be in relatively monodisperse state, which would be difficult for Au NPs to realize the capture or interaction process. On the other hand, ZnPc-COOH in high concentration would inevitably lead to aggregation owing to the π–π interaction between phthalocyanine rings, which would compete with the electrostatic interaction between ZnPc-COOH and Au NPs and the unchanged absorption peak at 534 nm was detected as a result of relative weak electrostatic interaction. The same phenomenon was also observed on the other two ZnPc-COOH aqueous solution as displayed in Fig. 3b, c the ZnPc-COOH-10

aqueous solution adopted in the interaction with Au NPs were denoted as ZnPc-COOH-10-1 (0.006 mg mL^{-1}), ZnPc-COOH-10-2 (0.012 mg mL^{-1}), ZnPc-COOH-10-3 (0.024 mg mL^{-1}), ZnPc-COOH-10-4 (0.048 mg mL^{-1}), and the ZnPc-COOH-10 aqueous solution involved were denoted as ZnPc-COOH-20-1 (0.004 mg mL^{-1}), ZnPc-COOH-20-2 (0.008 mg mL^{-1}), ZnPc-COOH-20-3 (0.016 mg mL^{-1}), ZnPc-COOH-20-4 (0.032 mg mL^{-1}). Different from ZnPc-COOH-6, the concentration and peak-shift diagram in Fig. 3d indicated that the most stable aggregate Au NPs/ZnPc-COOH-10 was generated with ZnPc-COOH-10-2 (0.012 mg mL^{-1}) along with a red shift of 18 nm, while the ZnPc-COOH-20-2 (0.008 mg mL^{-1}) promoted more obvious red-shift of 28 nm as shown in Fig. 3e, f, respectively. It was clearly that both the concentration and ring content of ZnPc-COOH have made a big difference to the formation of Au NPs/ZnPc-COOH hybrid complex, thus the adjustable microstructure and detectable aggregation extent would made Au NPs/ZnPc-COOH hybrid complex desirable in colorimetric sensing field.

On account of that the carboxyl group possessed coordination ability with various metal ions, the water-soluble carboxylated ZnPc-COOH was considered to be potential in coordinating with metal ions [9]. As mentioned above, the Au NPs has taken a significant role in colorimetric detection, which was realized via the change in color and the shifting of LSPR speak. Thus, the Au NPs/ZnPc-COOH hybrid complex would be potential in detecting metal ions, and the conjugate Au NPs/ZnPc-COOH-10-2 was selected to conduct the next exploration. Herein, metal ions including Al^{3+}, Cu^{2+}, Fe^{2+}, Fe^{3+}, Pb^{2+}, Ag^{+}, K^{+}, Na^{+}, Hg^{+}, Mg^{2+}, Ca^{2+}, Li^{+} of 0.1 M has been involved to examine the sensing selectivity of Au NPs/ZnPc-COOH hybrid complex, respectively. As shown in Fig. 4a, the LSPR band of Au NPs/ZnPc-COOH hybrid complex at 552 nm slightly moved to 625 nm in the presence of Ca^{2+}, leading to a color change from purple to blue, as illustrated in Fig. 4b, while all of the other metal ions showed considerably limited coordination ability and almost make no difference to the absorbance of Au NPs/ZnPc-COOH hybrid complex. Even though the Mg^{2+} has induced a relatively obvious shift from 552 to 580 nm of Au NPs/ZnPc-COOH hybrid complex along with a color intensity change from purple to dark purple, its high detection concentration made it uncompetitive as the sensitively detecting candidate. To evaluate the

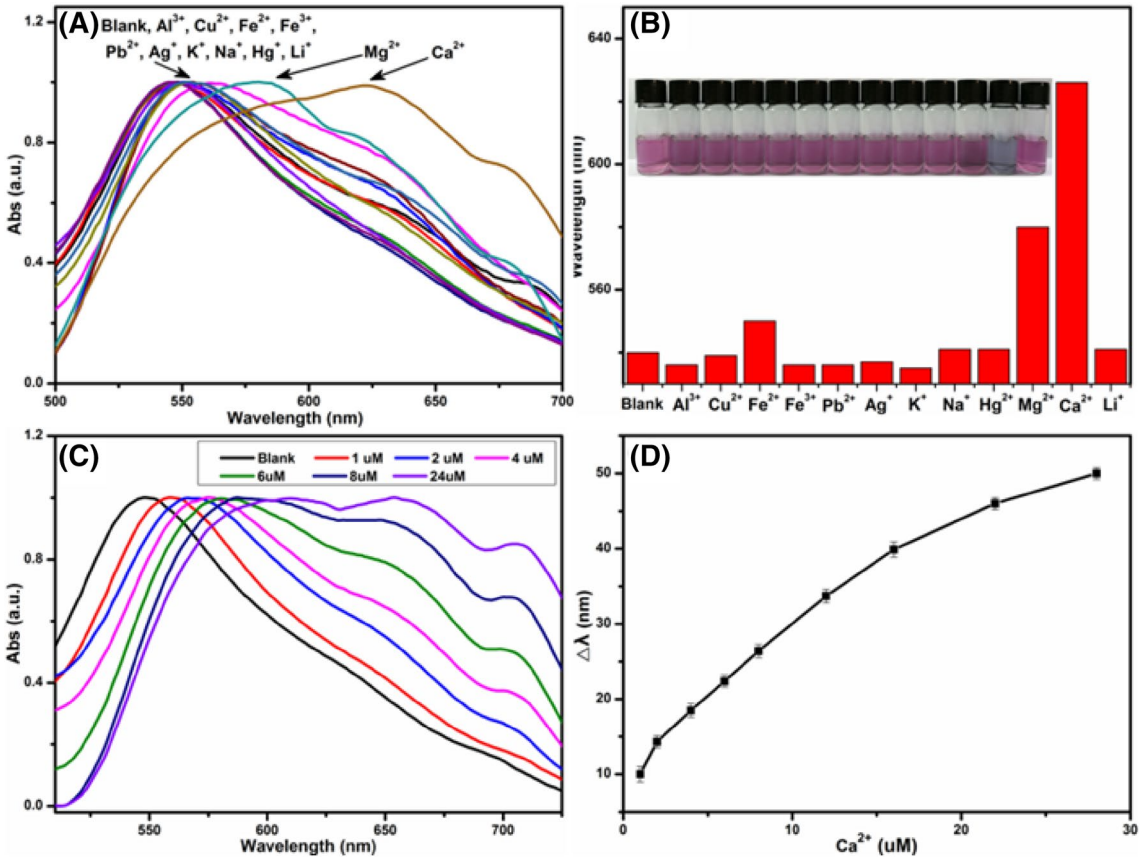

Fig. 4 The UV–Vis absorption spectra (**a**) and histogram spectra (**b**) of the colorimetric sensing of Au NPs/ZnPc-COOH hybrid complex interacted with different metal ions. The UV–Vis absorption spectra Au NP/ZnPc-COOH hybrid complex in the presence of lower concentration of Ca^{2+} (**c**) and the variation of absorption shifts function of Ca^{2+} concentration and constructed calibration curve (**d**)

sensitivity of Au NPs/ZnPc-COOH hybrid complex, a series of low concentration Ca^{2+} was added to coordinate the hybrid complex and the relationship between absorption shift ($\Delta\lambda$) and Ca^{2+} concentration (C). As displayed in Fig. 4c, as the Ca^{2+} concentration increased, the higher absorption peak shifted to longer wavelength. Moreover, the dose-responsive variation in the range 2–8 μM was fitted by a linear regression equation of $\Delta\lambda = 10.6543 + 1.93830C$ with coefficient of $R^2 = 0.9956$ and the detection concentration as low as 1 μM were obtained by using UV–Vis spectroscopy, as shown in Fig. 4d.

4 Conclusion

A novel hybrid complex based on the electrostatic interaction between water soluble carboxylated zinc phthalocyanine (ZnPc-COOH) and gold nanoparticles (Au NPs), was designed to detect Ca^{2+} in aqueous solution. Firstly, we synthesized nitrile groups terminated ZnPc followed with a facile one-step hydrolysis reaction to obtain the negatively charged water soluble ZnPc-COOH, which exhibited a microscopic H-type aggregate morphology. Then, the Au NPs with cationic surfactant CTAB as stabilizer were prepared and then modified with ZnPc-COOH. The results indicated that the ring content and concentration of ZnPc-COOH were essential factors to formulate Au NPs/ZnPc-COOH hybrid complex, which can be further employed for colorimetric detection of metal ions. It was found that the Au NPs/ZnPc-COOH hybrid complex rapidly aggregated along with a purple-to-blue color change in the presence of Ca^{2+}, and this specific optical response can be employed for detection of trace concentration Ca^{2+} down to 1 μM. Although there is still a large room for sensitivity enhancement at present, the specific Ca^{2+} induced optical response unambiguously confirmed the self-assembling of Au NPs and carboxylated ZnPc, both are considered as powerful photonic agents in biomedicine application, can be effectively modulated by the physiologically important Ca^{2+}. In this sense, the current work would open the potential for future application of Au NPs/ZnPc complex in biomedicine.

Acknowledgements The authors gratefully thank the financial support from National Natural Science Foundation of China (Project No. 51403029), the Fundamental Research Funds for the Central Universities (ZYGX2016J040) and the Scientific Research Foundation for the Returned Overseas Chinese Scholars from State Education Ministry (LXHG5003).

References

1. G. de la Torre, C.G. Claessens, T. Torres, Phthalocyanines: old dyes, new materials. Putting color in nanotechnology. Chem. Commun. **20**, 2000–2015 (2007)
2. G. de la Torre, P. Vázquez, F. Agulló-López, T. Torres, Role of structural factors in the nonlinear optical properties of phthalocyanines and related compounds. Chem. Rev. **104**(9), 3723–3750 (2004)
3. N. Venkatramaiah, D.M.G.C. Rocha, P. Srikanth, F.A. Almeida Paz, J.P.C. Tomé, Synthesis and photophysical characterization of dimethylamine-derived Zn(II) phthalocyanines: exploring their potential as selective chemosensors for trinitrophenol. J. Mater. Chem. C **3**(5), 1056–1067 (2015)
4. Y. Cheng, A.C. Samia, J.D. Meyers, I. Panagopoulos, B. Fei, C. Burda, Highly efficient drug delivery with gold nanoparticle vectors for in vivo photodynamic therapy of cancer. J. Am. Chem. Soc. **130**(32), 10643–10647 (2008)
5. W. Song, C. He, Y. Dong, W. Zhang, Y. Gao, Y. Wu, Z. Chen, The effects of central metals on the photophysical and nonlinear optical properties of reduced graphene oxide-metal(II) phthalocyanine hybrids. Phys. Chem. Chem. Phys. **17**(11), 7149–7157 (2015)
6. Q. Liang, M. Zhang, Z. Zhang, C. Liu, S. Xu, Z. Li, Zinc phthalocyanine coupled with UIO-66 (NH_2) via a facile condensation process for enhanced visible-light-driven photocatalysis. J. Alloys Compd. **690**, 123–130 (2017)
7. A.B. Sorokin, Phthalocyanine metal complexes in catalysis. Chem. Rev. **113**(10), 8152–8191 (2013)
8. K. Jia, L. Pan, Z. Wang, L. Yuan, X. Zhou, Y. Huang, C. Wu, X. Liu, Morphology and photophysical properties of dual-emissive hyperbranched zinc phthalocyanines and their self-assembling superstructures. J. Mater. Sci. **51**(6), 3191–3199 (2015)
9. L. Pan, K. Jia, H. Shou, X. Zhou, P. Wang, X. Liu, Unification of molecular NIR fluorescence and aggregation-induced blue emission via novel dendritic zinc phthalocyanines. J. Mater. Sci. **52**(6), 3402–3418 (2016)
10. T.P. Mthethwa, S. Tuncel, M. Durmus, T. Nyokong, Photophysical and photochemical properties of a novel thiol terminated low symmetry zinc phthalocyanine complex and its gold nanoparticles conjugate. Dalton Trans. **42**(14), 4922–4930 (2013)
11. Z. Huang, L. Huang, Y. Huang, Y. He, X. Sun, X. Fu, X. Xu, G. Wei, D. Chen, C. Zhao, Phthalocyanine-based coordination polymer nanoparticles for enhanced photodynamic therapy. Nanoscale **9**(41), 15883–15894 (2017)
12. P. Krystynik, P. Kluson, S. Hejda, D. Buzek, P. Masin, D.N. Tito, Semi-pilot scale environment friendly photocatalytic degradation of 4-chlorophenol with singlet oxygen species—direct comparison with H_2O_2/UV-C reaction system. Appl. Catal. B **160–161**, 506–513 (2014)
13. F. Dumoulin, M. Durmuş, V. Ahsen, T. Nyokong, Synthetic pathways to water-soluble phthalocyanines and close analogs. Coord. Chem. Rev. **254**(23–24), 2792–2847 (2010)
14. Y. Peng, H. Zhang, H. Wu, B. Huang, L. Gan, Z. Chen, The synthesis and photophysical properties of zinc(II) phthalocyanine bearing poly(aryl benzyl ether) dendritic substituents. Dyes Pigment. **87**(1), 10–16 (2010)
15. S. Tuncel, F. Dumoulin, J. Gailer, M. Sooriyaarachchi, D. Atilla, M. Durmus, D. Bouchu, H. Savoie, R.W. Boyle, V. Ahsen, A set of highly water-soluble tetraethyleneglycol-substituted Zn(II) phthalocyanines: synthesis, photochemical and photophysical properties, interaction with plasma proteins and in vitro phototoxicity. Dalton Trans. **40**(16), 4067–4079 (2011)
16. T. Nyokong, Effects of substituents on the photochemical and photophysical properties of main group metal phthalocyanines. Coord. Chem. Rev. **251**(13–14), 1707–1722 (2007)
17. X. Li, X. He, A.C.H. Ng, C. Wu, D.K.P. Ng, Influence of surfactants on the aggregation behavior of water-soluble dendritic phthalocyanines. Macromolecules **33**(6), 2119–2123 (2000)
18. K. Jia, X. Zhou, L. Pan, L. Yuan, P. Wang, C. Wu, Y. Huang, X. Liu, Plasmon enhanced fluorescence of a bisphthalonitrile-based dye via a dopamine mediated interfacial crosslinking reaction on silver nanoparticles. RSC Adv. **5**(88), 71652–71657 (2015)

19. J. Chen, N. Chen, J. Huang, J. Wang, M. Huang, Derivatizable phthalocyanine with single carboxyl group: synthesis and purification. Inorg. Chem. Commun. **9**(3), 313–315 (2006)
20. X. Zhou, X. He, S. Wei, K. Jia, X. Liu, Au nanorods modulated NIR fluorescence and singlet oxygen generation of water soluble dendritic zinc phthalocyanine. J. Colloid Interface Sci. **482**(Supplement C), 252–259 (2016)
21. F. Setaro, R. Ruiz-Gonzalez, S. Nonell, U. Hahn, T. Torres, Synthesis, photophysical studies and (1)O(2) generation of carboxylate-terminated zinc phthalocyanine dendrimers. J. Inorg. Biochem. **136**, 170–176 (2014)
22. K. Saha, S.S. Agasti, C. Kim, X. Li, V.M. Rotello, Gold nanoparticles in chemical and biological sensing. Chem Rev. **112**(5), 2739–2779 (2012)
23. J.F. Zhang, Y. Zhou, J. Yoon, J.S. Kim, Recent progress in fluorescent and colorimetric chemosensors for detection of precious metal ions (silver, gold and platinum ions). Chem. Soc. Rev. **40**(7), 3416–3429 (2011)
24. A. Corma, H. Garcia, Supported gold nanoparticles as catalysts for organic reactions. Chem. Soc. Rev. **37**(9), 2096–2126 (2008)
25. M.-C. Daniel, D. Astruc, Gold nanoparticles: assembly, supramolecular chemistry, quantum-size-related properties, and applications toward biology, catalysis, and nanotechnology. Chem. Rev. **104**(1), 293–346 (2004)
26. E. Blanco, H. Shen, M. Ferrari, Principles of nanoparticle design for overcoming biological barriers to drug delivery. Nat. Biotechnol. **33**, 941 (2015)
27. E. Priyadarshini, N. Pradhan, Gold nanoparticles as efficient sensors in colorimetric detection of toxic metal ions: a review. Sens. Actuators B **238**, 888–902 (2017)
28. P.K. Jain, K.S. Lee, I.H. El-Sayed, M.A. El-Sayed, Calculated absorption and scattering properties of gold nanoparticles of different size, shape, and composition: applications in biological imaging and biomedicine. J. Phys. Chem. B. **110**(14), 7238–7248 (2006)
29. P. Wang, Z. Lin, X. Su, Z. Tang, Application of Au based nanomaterials in analytical science. Nano Today **12**, 64–97 (2017)
30. H. Jans, Q. Huo, Gold nanoparticle-enabled biological and chemical detection and analysis. Chem. Soc. Rev. **41**(7), 2849–2866 (2012)
31. H. Sharma, N. Kaur, A. Singh, A. Kuwar, N. Singh, Optical chemosensors for water sample analysis. J. Mater. Chem. C **4**(23), 5154–5194 (2016)
32. L. Li, B. Li, Sensitive and selective detection of cysteine using gold nanoparticles as colorimetric probes. Analyst **134**(7), 1361–1365 (2009)
33. J. Zhang, Y. Wang, X. Xu, X. Yang, Specifically colorimetric recognition of calcium, strontium, and barium ions using 2-mercaptosuccinic acid-functionalized gold nanoparticles and its use in reliable detection of calcium ion in water. Analyst **136**(19), 3865–3868 (2011)
34. S. Kim, J.W. Park, D. Kim, D. Kim, I.H. Lee, S. Jon, Bioinspired colorimetric detection of calcium(II) ions in serum using calsequestrin-functionalized gold nanoparticles. Angew. Chem. **48**(23), 4138–4141 (2009)
35. B. Nikoobakht, M.A. El-Sayed, Preparation and growth mechanism of gold nanorods (NRs) using seed-mediated growth method. Chem. Mater. **15**(10), 1957–1962 (2003)